PHYSICAL REVIEW A VOLUME 21, NUMBER 5 MAY 1980

Density-functional theory of positronium and electron bubbles in helium fluids

R. M. Nieminen,* I. Välimaa, M. Manninen, and P. Hautojärvi
Department of Technical Physics, Helsinki University of Technology, SF-02150 Espoo 15, Finland
(Received 17 September 19)

The density-functional method is applied to excess electrons and positronium atoms in helium fluids. The self-trapping is investigated in a fully self-consistent fashion, and formulas are given for the particle energy and Ps pick-off annihilation rate in quasifree as well as localized states. The numerical results compare well with experimental data. However, the need for a more sophisticated treatment of threshold effects near the onset of bubble formation is indicated.

I. INTRODUCTION

Density-functional ideas have gained wide popularity and have met with considerable success in a number of quantum problems in atomic, molecular, and solid-state physics. They provide a powerful method to describe situations where *both* the interactions between particles *and* self-consistency are important. Applications which are especially appealing include various impurity and defect properties of metals with the nonuniformity of the electron system playing an essential role (see, for example, Lang,[1] Gunnarsson, and Lundqvist[2] and references therein). There have also recently been other interesting applications, e.g., Mott-type transitions in doped semiconductor materials.[3]

A few years ago Ebner, Saam, and Stroud[4] formulated the problem of an inhomogeneous *classical* fluid on the basis of density-functional theory, which, though remarkably simple and transparent, yielded encouraging results for the surface properties of rare gas liquids. There is a family of other interesting and experimentally accessible cases of a nonuniform classical system; the inhomogeneities induced by excess particles immersed in a fluid. In the case of a monatomic fluid, positively charged particles cause the accumulation of the host atoms in their vicinity due to the attractive electrostrictive forces; excess negatively charged particles may dig a cavity around them due to the increased exchange repulsion. Especially interesting are the cases when the foreign particles behave quantum mechanically: This happens with injected electrons, positrons, and positronium (Ps) atoms. For these light particles one can view the situation as a competition between localized and extended behavior. At a certain temperature and density range the free energy of the total system is minimized when the excess particle wave function is localized in space with an associated static fluctuation of the host fluid density; the particle is self-trapped. This phenomenon was first suggested by Ferrell[5] to account for the anomalously slow decay rate of ortho-Ps in liquid helium.

For electrons, there exists a body of evidence for such states in a number of nonpolar fluids, both liquid and gaseous. An electron in such a localized state is characterized by a mobility several orders of magnitude smaller than that in a quasifree conduction band state. For a review, see Davis and Brown.[6] The self-trapping has recently been demonstrated for positrons in low-temperature gaseous He.[7-9] One may think of the positrons as inducing droplet formation or a "local" gas-liquid phase transition near the critical point where the gas density can be increased without essentially increasing the free energy.

The excess electrons have provided considerable information about the localization mechanism as well as the excitations (scattering mechanisms) in the host fluid, including superfluidity aspects, via mobility measurements.[10] Yet the information about the "bubble" or "snowball" structure itself is only indirect. On the other hand, the positron- and Ps-induced density fluctuations are readily accessible by annihilation-rate measurements and provide stringent tests for theories of the structure of the self-trapped state.

In this paper we report detailed calculations, based on the density-functional scheme, of the electron and Ps bubbles in fluid helium. Our work on the electron bubble is somewhat parallel to that of Ebner and Punyanitya,[11] who deal with a number of rare gases at relatively high temperatures. Their paper also contains a comprehensive list of references to earlier related work. As for Ps bubbles, our method transcends the work of Hernandez[12] on liquid He and of Iakubov and Khrapak[13] on rare gases. From fully self-consistent solutions of the relevant Euler-Lagrange equations we obtain the stability regions of bubble formation and density profiles at different densities and temperatures. For Ps bubbles we calculate the pick-off annihilation rate as a function of density and temperature and compare them with the recent ex-

perimental results.[14]

The paper is organized as follows. In Sec. II we briefly review the density-functional theory of nonuniform classical fluids together with the basic equations for self-trapping phenomena. In Sec. III we discuss the energy of a quasifree particle in a uniform fluid. Section IV deals with electron bubbles, and Sec. V with Ps bubbles. Section VI contains the conclusions.

II. DENSITY-FUNCTIONAL THEORY OF NONUNIFORM CLASSICAL FLUIDS

Consider a classical system of particles with a fixed chemical potential μ at temperature T subject to a local external potential $V(\vec{r})$. The essential ingredient in the density-functional theory is the grand free energy $\Omega[n]$, which possesses the minimal property with respect to variations of the number density $n(\vec{r})$ in the equilibrium state.

In the case of a foreign quantum-mechanical particle interacting with the fluid, the external potential is

$$V(\vec{r})=\int d\vec{r}'v(\vec{r}-\vec{r}')\,|\psi(\vec{r}')|^2\,, \tag{1}$$

where $v(\vec{r})$ is the particle-atom potential, assumed to be local, and $|\psi|^2$ is the probability density for the injected particle (mass M). Following Ebner, Saam, and Stroud,[4] we write the grand free energy as a functional:

$$\Omega[n;\psi]=\int d\vec{r}[f(n(\vec{r}))-\mu n(\vec{r})]+\int d\vec{r}\,V(\vec{r})n(\vec{r}) +\frac{kT}{4}\int d\vec{r}\int d\vec{r}'c(\vec{r},\vec{r}')[n(\vec{r})-n(\vec{r}')]^2 +\int d\vec{r}\frac{\hbar^2}{2M}|\nabla\psi(\vec{r})|^2\,, \tag{2}$$

which is minimized with respect to variations of $n(\vec{r})$ and $\psi(\vec{r})$. Above, $f(n)$ is the Helmholtz free-energy density and $c(\vec{r},\vec{r}')$ is the Ornstein-Zernlike direct correlation function generalized to the nonuniform system. A remarkably good approximation to $c(\vec{r},\vec{r}')$ is[4]

$$c(\vec{r},\vec{r}')=c(|\vec{r}-\vec{r}'|;\bar{n}) \tag{3}$$

with

$$\bar{n}=[n(\vec{r})+n(\vec{r})]/2\,.$$

Minimizing with respect to a normalizable ψ, one finds the Schrödinger equation

$$-(\hbar^2/2M)\nabla^2\psi(\vec{r})+\tilde{V}(\vec{r})\psi(\vec{r})=\epsilon\psi(\vec{r})\,, \tag{4}$$

where

$$\tilde{V}(\vec{r})=\int d\vec{r}'n(\vec{r}')v(\vec{r}-\vec{r}')\,. \tag{5}$$

As $r\to\infty$, the density goes to a constant n_0 and $\tilde{V}(\vec{r})$ approaches the energy whereby the uniform background medium shifts the energy of the particle

$$\tilde{V}(\vec{r})\xrightarrow[r\to\infty]{}E_\infty(n_0)\,. \tag{6}$$

If the density variations are slow in the scale where the two-body potential changes rapidly, one may apply the local density approximation; i.e.,

$$\tilde{V}(\vec{r})=E_\infty(n(\vec{r}))\,, \tag{7}$$

which is expected to be very good for the problems considered here. It should be noted that ψ is not strictly speaking the full particle wave function, but a kind of pseudo-wave function, which reflects the changes in the average particle distribution, and does not have any detailed structure near individual fluid atoms. The full wave function in a homogeneous fluid and the related energy $E_\infty(n_0)$ will be determined in the next section.

Minimizing now Ω with respect to n, we find the integral equation

$$\mu(n(\vec{r}))+\frac{kT}{4}\int d\vec{r}'\left(\frac{\partial c(|\vec{r}-\vec{r}'|;\bar{n})}{\partial\bar{n}}[n(\vec{r})-n(\vec{r}')]^2+4c(|\vec{r}-\vec{r}'|;n)[n(\vec{r})-n(\vec{r}')]\right)=\mu(n_0)-\frac{\partial E_\infty(n(\vec{r}))}{\partial n}|\psi(\vec{r})|^2\,. \tag{8}$$

We are mainly interested in the free-energy difference between the localized state and the quasifree state in a uniform fluid. The change in the grand potential due to self-trapping is

$$\Delta\Omega=\Omega[n;\psi]-\Omega[n_0] =\int d\vec{r}[f(n(\vec{r}))-f(n_0)]+\frac{kT}{4}\int d\vec{r}\int d\vec{r}'c(|\vec{r}-\vec{r}'|;\bar{n})[n(\vec{r})-n(\vec{r}')]^2+\mu(n_0)\int d\vec{r}[n(\vec{r})-n_0]+E_B\,, \tag{9}$$

where $|E_B|=|\epsilon-E_\infty(n_0)|$ is the particle binding energy in its self-trapped state [see Eq. (4)]. At a given temperature T and fluid density n_0, the self-consistent solution of Eqs. (4) and (8) gives the ground-state wave function and the associated fluid density profile $n(\vec{r})$. The self-trapped state is stable if a minimum is found with $\Delta\Omega<0$; however, there may also exist minimal solutions with $\Delta\Omega>0$. These are metastable localized states.

III. PARTICLE DISTRIBUTION AND ENERGY IN A UNIFORM FLUID

Consider a particle immersed in a uniform reference fluid, which does not respond to its presence. The interaction between the particle and individual fluid atoms in a neutral system is short ranged. Near the atomic cores $v(\vec{r})$ is large due to orthogonalization repulsion for electrons and Ps, whereas the nuclear Coulomb potential repels positrons. At larger distances there is a weak minimum whereafter the potential approaches the van der Waals limit proportional to $-r^{-4}$ for charged particles and to $-r^{-6}$ for neutral atoms. The total potential experienced by the particle can in an instantaneous atomic configuration be expressed as

$$V_p(\vec{r})=\sum_n v(\vec{r}-\vec{R}_n)\,, \tag{10}$$

where the sum goes over the atomic positions $\vec{R}_n$. The ground-state wave function obeys

$$-(\hbar^2/2M)\nabla^2\psi_0(\vec{r})+V_p(\vec{r})\psi_0(\vec{r})=E_\infty\psi_0(\vec{r})\,. \tag{11}$$

The wave-function amplitude is largest in the interatomic regions and dies off quickly on approach to the fluid atoms. Following the original ideas of Stott[15,16] for positron distribution in solids, we explicitly account for the core repulsion by writing ψ_0 in a product form

$$\psi_0(\vec{r})=\sum_n u_0(\vec{r}-\vec{R}_n)\phi(\vec{r})\,, \tag{12}$$

where u_0 is a solution to the "cellular" equation

$$-(\hbar^2/2M)\nabla^2u_0(\vec{r})+v(\vec{r})u_0(\vec{r})=E_0u_0(\vec{r})\quad(r<R_0) \tag{13}$$

subject to the boundary condition

$$\nabla u_0(\vec{r})\big|_{R_0}=0\,. \tag{14}$$

Above, R_0 is a cell radius, which is conveniently chosen as

$$R_0=(3/4\pi n_0)^{1/3}\,. \tag{15}$$

u_0 is a Wigner-Seitz wave function and E_0 the corresponding energy. By substitution into Eq. (11) one finds the following equation for the envelope "pseudo-wave function" $\phi(\vec{r})$:

$$-(\hbar^2/2M)\nabla^2\phi(\vec{r})+W(\vec{r})\phi(\vec{r})=E_\infty\phi(\vec{r})\,, \tag{16}$$

with the "pseudopotential"

$$\begin{aligned}W(\vec{r})&=V_p(\vec{r})-v(\vec{r}-\vec{R}_n)+E_0\\&\quad-(\hbar^2/M)\nabla\ln u_0(\vec{r})\vec{r}\cdot\nabla\quad(|\vec{r}-\vec{R}_n|<R_0)\\&=V_p(\vec{r})\quad(|\vec{r}-\vec{R}_n|>R_0)\end{aligned} \tag{17}$$

which is much weaker than the original v. Inside a particular cell, W is small due to the near cancellation of V_p and v, the main effect being absorbed in the Wigner-Seitz solution. Outside the cell the potential $v(\vec{r})$ dies off quickly. The boundary conditions (14) and (15) are useful since they make effective use of the implicit assumption of a uniform, on an average homogeneous system. An accurate solution to Eq. (16) may be obtained from second-order perturbation theory as

$$\phi(\vec{r})=C\left[e^{i\vec{p}\cdot\vec{r}}-\frac{2M}{\hbar^2}\sum_{k\neq p}\frac{\langle\vec{k}|W|\vec{p}\rangle}{k^2-p^2}e^{i\vec{k}\cdot\vec{r}}\right], \tag{18}$$

$$E_\infty=\frac{\hbar^2p^2}{2M}+\langle\vec{p}|W|\vec{p}\rangle-\frac{2M}{\hbar^2}\sum_{k\neq p}\frac{\langle\vec{k}|W|\vec{p}\rangle\langle\vec{p}|W|\vec{k}\rangle}{k^2-p^2}\,. \tag{19}$$

C is a normalizing constant. The matrix elements in Eqs. (18) and (19) may be written as

$$\langle\vec{k}|W|\vec{p}\rangle=n_0S(q)[\omega(q)-(\hbar^2/M)\vec{p}\cdot\vec{q}B(q)]\,, \tag{20}$$

where

$$\vec{q}=\vec{p}-\vec{k}\,,$$

$$\omega(q)=4\pi\int_{R_0}^{\infty}dr\,r^2v(r)\frac{\sin qr}{qr}+4\pi R_0^2E_0\frac{j_1(qR_0)}{q}\,, \tag{21}$$

$$B(q)=-\frac{\hbar^2}{M}4\pi\int_0^{R_0}dr\,r^2\ln u_0(r)\frac{\sin qr}{qr}\,, \tag{22}$$

and $S(q)$ is the structure factor carrying the information about the atomic positions. We have normalized u_0 so that $u_0(R_0)=1$. Inserting into Eq. (19) and averaging over the atomic sites in the spirit of the Born-Oppenheimer approximation one finds in the thermodynamic limit

$$E_\infty(n_0)=\frac{\hbar^2p^2}{2M}+E_0+4\pi n_0\int_{R_0}^{\infty}dr\,r^2v(r)-\frac{Mn_0}{\pi^2\hbar^2}\int_0^{\infty}dk\,\omega(k)S_L(k)[\omega(k)+k^2B(k)]\,, \tag{23}$$

where $S_L(k)$ is the *fluid* structure factor, determined by the direct correlation function $c(r;n)$. Normally we are interested in states near the bottom of the conduction band where $\hbar^2p^2/2M=3kT/2$ is negligible.

The method outlined above is completely general and contains, in an approximate way, the multiple-scattering contributions to the particle energy. It is easy to see that it approaches the optical potential limit

$$E_\infty(n_0)\to(2\pi\hbar^2/M)an_0 \tag{24}$$

at low densities (a is the scattering length), with the nonlinearities playing an increasingly important role at higher densities. Below we will apply the above formulas to electrons and Ps atoms in

helium fluids.

To proceed one has to specify the temperature and density dependence of the direct correlation function $c(r;n)$ which determines via the compressibility equation of state[17] the thermodynamic functions $f(n)$ and $\mu(n)$. For example, one can determine c by solving the Percus-Yevick equation with the host fluid interatomic potential.[4] A particularly simple and for our purposes useful model is the hard-sphere Percus-Yevick solution, which can be obtained analytically.[17]

IV. ELECTRON BUBBLES

The electron-helium interaction has been taken from the work of Kestner *et al.*[18] It consists of a Hartree term, an exchange repulsion term, and an attractive polarization part. It has an s-wave scattering length of 0.629 Å in agreement with the experimental value.[19]

Figure 1 shows the density dependence of the E_∞ for electrons in helium. Here we have used the hard-sphere liquid structure factor in Eq. (23) with the hard-sphere diameter $\sigma = 2.556$ Å coinciding with the node in the conventional Lennard-Jones potential for He. For comparison, we have also shown the optical potential and the perturbative result of Tankersley.[20]

The density-temperature curve that marks the boundary of stable ($\Delta\Omega < 0$) self-trapped electron states in fluid helium is drawn in Fig. 2. Here, again, the Percus-Yevick hard-sphere approximation has been used for the host fluid structure

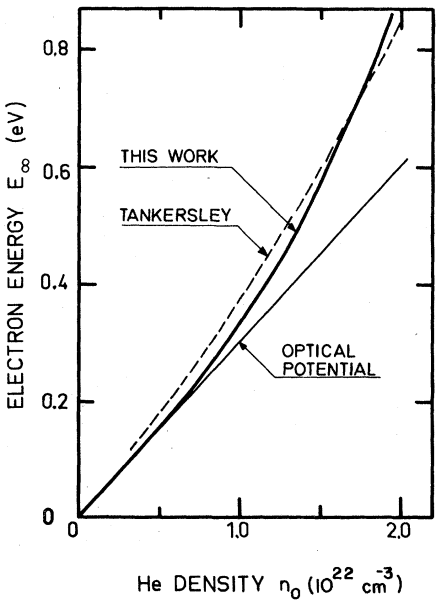

FIG. 1. The energy of a delocalized excess electron in uniform helium fluid. The optical potential Eq. (24) and the results of Tankersley (Ref. 20) are also shown.

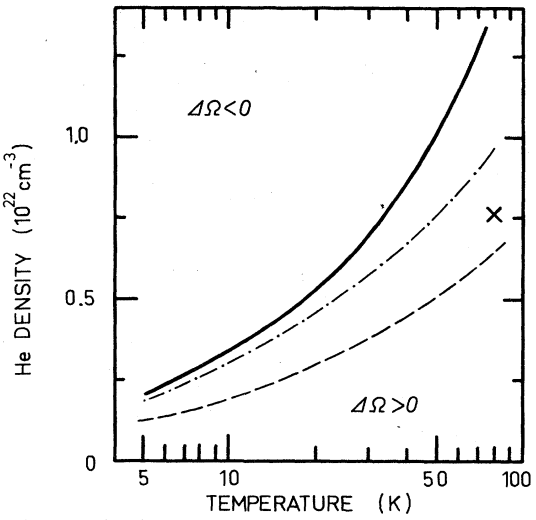

FIG. 2. The density-temperature curve for the boundary of stable self-trapped electron states in fluid helium (full curve). The dash-dotted line is the ideal gas result (Ref. 22) corresponding to our $E_\infty(n)$. The cross is the single point calculated by Ebner and Punyanitya (Ref. 11); the dashed line is the result of Hernandez (Ref. 21).

factor. To see the effect of the equation of state we have also included the ideal gas result[22] modified to our $E_\infty(n)$. As expected, at low densities (low temperatures) the difference vanishes but becomes significant at liquid densities. For comparison, we have also included the result of Hernandez,[21] based on the ideal gas approximation and the hard-sphere Wigner-Seitz model for $E_\infty(n)$. The large difference between the two ideal gas results is solely due to the difference in $E_\infty(n)$, demonstrating the sensitivity of the result to electron-helium interaction in the medium. The hard-sphere Wigner-Seitz result for $E_\infty(n)$ is larger and increases more rapidly with density resulting in stable bubble formation at lower densities.

Ebner and Punyanitya[11] have calculated the critical density for bubble formation at one temperature using a density-functional approach with the Percus-Yevick $c(r;n)$ calculated from the He-He Lennard-Jones interaction, and Hernandez's $E_\infty(n)$. This single point is also shown in Fig. 2. The difference from our hard-sphere result is mainly due to the different $E_\infty(n)$, but partly also reflects the fact that the hard-sphere equation of state overestimates the pressure at high densities and temperatures.

The experimental determination of the phase boundary for electron bubble formation is not quite straightforward. Hernandez[21] has estimated the boundary by determining from isothermal mobility measurements the density points where the mobility is one hundredth and one tenth of the semiclassical mobility for electrons in extended states.

If the mobility drop by a factor of 100 is associated with the phase boundary, the experimental result lies between our results (the full curve) and that of Hernandez, whereas a mobility drop by a factor of 10 gives a phase boundary which is below Hernandez's result in Fig. 2.

As has been discussed by several authors[11,21,23] the free-energy expression (2) attributes no entropy to the excess particle. The main contribution to this arises from the translational degrees of freedom of the bubble. If these are included, the free-energy difference is lowered by the amount

$$\Delta\Omega_e = -\tfrac{3}{2}kT \ln\left(\frac{M^*}{M}\right), \tag{25}$$

where M^* is the translational effective mass of the bubble. The effect would be to convert a number of metastable self-trapped states to stable, thereby lowering the curves in Fig. 2. We shall return to this question in the context of Ps bubbles in the next section.

A set of typical density profiles for the electron bubble is shown in Fig. 3. The number of displaced helium atoms $N = \int d\vec{r}\,[n_0 - n(\vec{r})]$ and the effective bubble radius $R = (3N/4\pi n_0)^{1/3}$ are shown in Figs. 4 and 5 as functions of temperature and density. With increasing temperature, the bubble size decreases and the profiles become more diffuse.

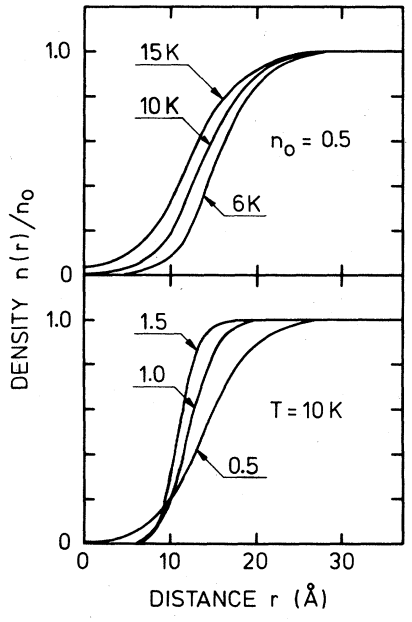

FIG. 3. Density profiles for electron bubbles in helium at various temperatures and densities. Upper part: Fixed density $n_0 = 0.5 \times 10^{22}$ cm^{-3} with temperatures $T = 6$, 10, and 15 K. Lower part: Fixed temperature $T = 10$ K with densities $n_0 = 0.5$, 1.0, and 1.5×10^{22} cm^{-3}.

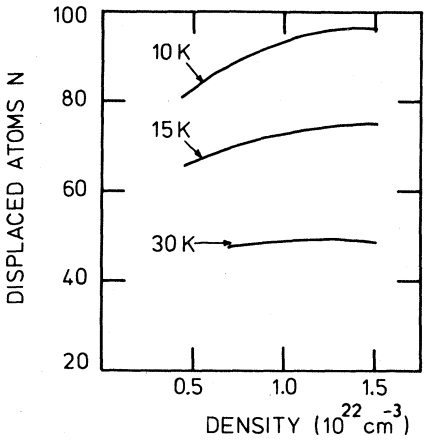

FIG. 4. The number of displaced atoms for electron bubbles in helium fluid as a function of density at various temperatures.

V. POSITRONIUM IN HELIUM

We now come to our principal concern, the behavior of positronium atoms in dense rare gases. During the slowing down the positron can capture an electron and form a positronium atom, either in the para or in the ortho state. The 2γ annihilation of the parapositronium occurs with a lifetime of 0.125 ns, whereas in the ortho state this is forbidden. Therefore, in vacuum the orthopositronium decays into 3 γ quanta with a very long lifetime of 142 ns.[24] In condensed matter the positron of the orthopositronium atom overlaps with electrons of opposite spins in the surrounding medium and the 2γ annihilation by this pick-off process reduces the long lifetime usually to a few nanoseconds. In liquid helium, however, an anomalously long lifetime of about 100 ns was found by Paul and Graham[25] and by Wackerly and Stump.[26] Ferrell[5]

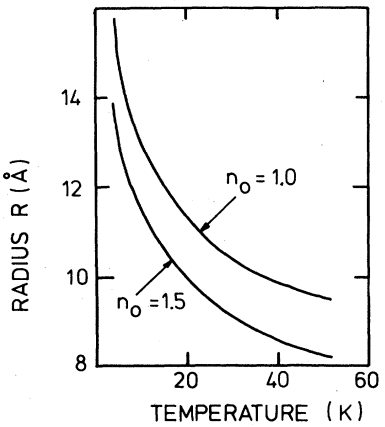

FIG. 5. The effective radius for electron bubbles in helium fluid as a function of temperature at two densities $n_0 = 1.0$ and 1.5×10^{22} cm^{-3}.

explained this to be due to an orthopositronium inside a bubblelike cavity, in which case the overlap of the positron wave function with electrons of the helium liquid is reduced.

Later experiments have shown that positronium exists in the bubble state also in gaseous and solid phases of helium.[27-29] From the lifetime and angular correlation measurements it has been possible to extract information on the radius and potential depth of the bubble described by a simple square-well model.[27-32] There is also evidence that a Ps bubble is formed in Ne, Xe, H_2, but perhaps not in Ar.[30,33,34]

A. Pick-off annihilation rate in a uniform fluid

The pick-off annihilation rate of the ortho-Ps is proportional to the overlap of its wave function with the fluid atom electron clouds. For a quasi-free Ps in a uniform fluid the pick-off rate is

$$\lambda_\infty(n_0) = 4\pi r_0^2 \lambda^1 Z_{eff} \times \left\langle \int d\vec{r}\, |\psi_0(\vec{r})|^2 \sum_n \rho_c(\vec{r} - \vec{R}_n) \right\rangle, \tag{26}$$

where r_0 is the classical electron radius, c is the velocity of light, and $\rho_c(\vec{r} - \vec{R}_n)$ is the electron density due to an atom at $\vec{R}_n$. The brackets denote a thermal average; ψ_0 is the full Ps center-of-mass wave function. Electron-positron correlation is of course very important in determining the absolute value of the annihilation rate. It is, however, a basically atomic process and does not depend on the fluid environment. Its effect is absorbed in $^1Z_{eff}$, to which we use the experimental low-density value of 0.129.[27]

At the densities of interest here it is perfectly reasonable to assume that the atomic electron clouds do not extend further than the cell radius: i.e., $\rho_c(r) = 0$ for $r > R_0$. Then one may proceed as in Sec. III by separating a core part and a modulating envelope in the Ps wave function and one finds (cf. Stott and West[16])

$$\lambda_\infty(n_0) = \frac{4\pi r_0^2 c\, {}^1Z_{eff}}{1/n_0 - \chi(0)} \times \frac{\sigma(0)\left(1 - \frac{2M}{\hbar^2\pi^2}\int_0^\infty dk\, \omega(k) S_L(k) \frac{\sigma(k)}{\sigma(0)}\right)}{1 + \frac{2M}{\hbar^2\pi^2}\int_0^\infty dk\, \omega(k) S_L(k) \frac{\chi(k)}{1/n_0 - \chi(0)}}, \tag{27}$$

where

$$\sigma(k) = 4\pi \int_0^{R_0} dr\, r^2 u_0(r) \frac{\sin kr}{kr} \tag{28}$$

and

$$\chi(k) = 4\pi \int_0^{R_0} dr\, r^2 [1 - u_0^2(r)] \frac{\sin kr}{kr}. \tag{29}$$

Above, S_L is again the liquid structure factor, and the core part of the Ps center-of-mass wave function is normalized to $u_0(R_0) = 1$.

Equation (27) supersedes earlier approximate treatments of multiple scattering[5,29] for Ps annihilation. It accounts for the nonlinear excluded volume effects as the Ps is squeezed into the interatomic regions when density is increased.

B. Ps-He potential

It is reasonable to think of Ps as a composite particle with no internal structure apart from a nonzero polarizability, since the binding energy 6.8 eV is large compared to any other energy involved. However, an accurate Ps-He potential is difficult to construct and pick-off rate measurements do actually give useful information about the interaction, supplementing scattering experiments.

At large distances, the potential approaches the London limit and the asymptotic form is (in atomic units)

$$v(r) = -19.3/r^6. \tag{30}$$

At shorter distances, we tried to follow the prescriptions of Barker and Brandsen[35] and Fraser.[36] However, the resulting potential turned out too soft at its core, giving a pick-off rate $\lambda_\infty(n_0)$, which rose unphysically fast with increasing density. Consequently we decided to use a parametrized Lennard-Jones potential

$$v(r) = 4\epsilon\left[\left(\frac{\sigma}{r}\right)^{12} - \left(\frac{\sigma}{r}\right)^6\right]. \tag{31}$$

The asymptotic condition (30) fixes the product $4\epsilon\sigma^6$, while another condition may be obtained by requiring the potential to have a prechosen scattering length a. The dependence of the scattering length on σ is illustrated in Fig. 6. Estimated values for the Ps-He scattering length range between 0.50 and 0.80 Å,[27,28,37] whereby σ varies between 0.98 and 1.4 Å and ϵ between 44 000 and 4900 K. It is interesting to compare these values with the Lennard-Jones parameters estimated for H-He potential by Miller[38]; $\sigma = 3.2$ Å and $\epsilon = 6.6$ K. The asymptotic limits for these two cases are consistent since at the London limit

$$v \propto -\alpha_1\alpha_2 \frac{I_1 - I_2}{I_1 + I_2} \frac{1}{r^6}, \tag{32}$$

where the α's and I's are the polarizabilities and the ionization potentials of the two atoms, respectively. The Ps-polarizability is eight times that of hydrogen, while the ionization potential is half of the hydrogen value. On the other hand, the Ps-He potential has a much smaller repulsive core and consequently much larger ϵ indicating consider-

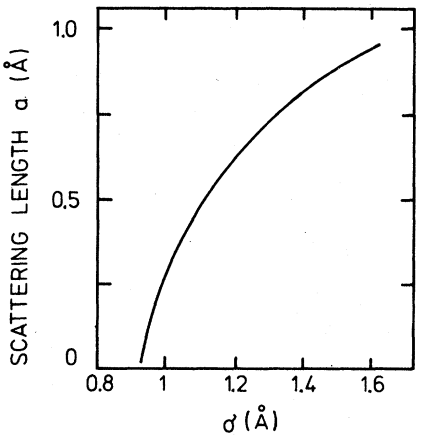

FIG. 6. The dependence of the scattering length a on the parameter σ of the Ps-He Lennard-Jones potential defined in Eq. (31).

ably stronger attractive interaction at intermediate distances than in the H-He potential.

Figure 7 shows the uniform fluid pick-off rate $\lambda_\infty(n_0)$ and the energy $E_\infty(n_0)$ as functions of density, calculated using the Lennard-Jones Ps-He interaction and the formulas (27) and (23). The liquid structure factor $S_L(k)$ is again the hard-sphere Percus-Yevick one, with a hard-core diameter of 2.556 Å. Note that the strong r^{-12} repulsion leads to a numerical divergence in the term $B(k)$ [Eq. (29)] involved in the energy calculation. This can be avoided by cutting off the potential to a finite constant at very small densities. For simplicity we have ignored the corresponding term in the energy as its effect is small.

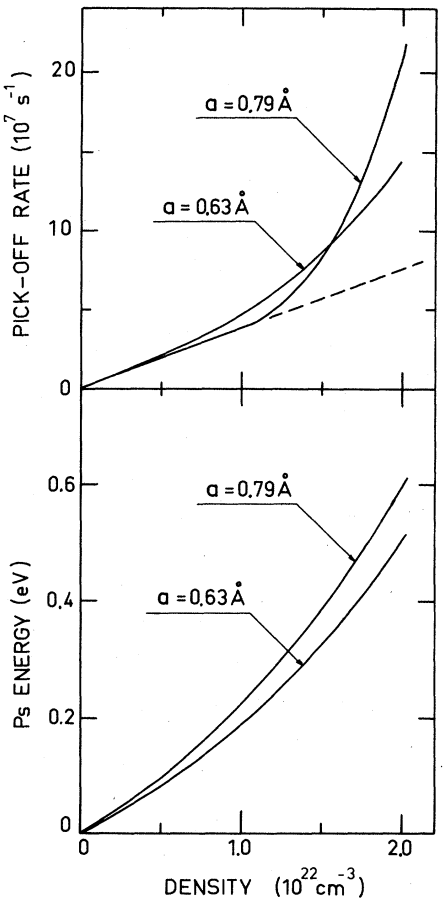

FIG. 7. The pick-off rate $\lambda_\infty(n_0)$ and the energy $E_\infty(n_0)$ of quasifree Ps as functions of density in uniform helium fluid at two different values for Ps-He scattering length.

C. Ps bubbles

The pick-off annihilation rate in the self-trapped state is

$$\lambda = \left\langle \int d\vec{r}\, \lambda_\infty(n(\vec{r}))\, |\psi(\vec{r})|^2 \right\rangle , \tag{33}$$

where the brackets denote a thermal average and ψ is the wave function [Eq. (4)] of the self-trapped state. In calculating the thermal average we have neglected the excited states of the bubble, which may be of several types. There are states with density profiles not minimizing Ω, which can simply be visualized as deformations or capillary excitations of the bubble. The density of such unstable but in principle populated states is difficult to estimate; yet they may be important near the threshold of bubble formation. From the Ps point of view, there are those for which the Ps center-of-mass is at rest with respect to the fluid. For typical bubble states with a radius of $R \approx 15$ Å, the Ps excitation energy $\approx \hbar^2/2MR^2$ is of the order of 300 K, much higher than temperatures considered here. Also we assume the Ps to be completely thermalized when annihilating. Thus practically none of these excited states are populated. There are also states in translational motion. They have a negative contribution to the free energy and may actually render metastable states stable. Thus one would expect them to be important near the onset of bubble formation (see below). Unfortunately, their quantitative treatment is very difficult.

Currently we approximate Eq. (33) by a two-state model

$$\lambda = [\lambda_\infty(n_0) e^{\Delta\Omega/kT} + \lambda_t] / (1 + e^{\Delta\Omega/kT}) , \tag{34}$$

where λ_t denotes the expression (33) evaluated in the bubble state.

Figure 8 shows calculated pick-off rates in helium as a function of density at varying temperatures. The onset of bubble formation is clearly visible as a departure from the linear dependence valid at low densities. The calculated curves cor-

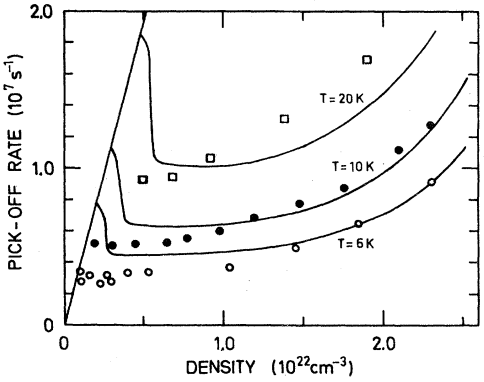

FIG. 8. Calculated pick-off annihilation rates for ortho-Ps as functions of helium density at various temperatures. The sharp drops represent the onset of bubble formation. The experimental points are from Ref. 14.

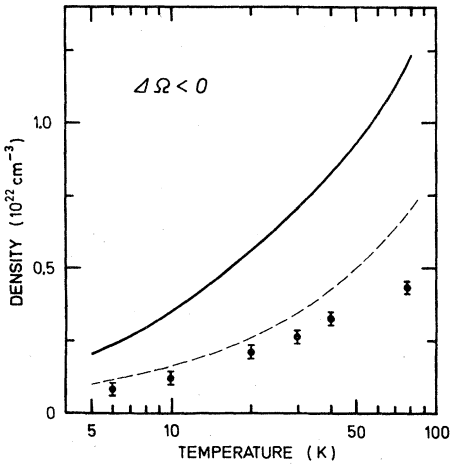

FIG. 9. Formation region of Ps bubbles in fluid helium. The solid line represents the theoretical result where $\Delta\Omega = 0$. The experimental points have been determined by extrapolating the pick-off rate in the bubble state to the straight line of the pick-off rate of quasifree Ps (Ref. 14). The dotted curve corresponds to the similar extrapolation of calculated pick-off rates. For details see text.

respond to a Ps-He scattering length of 0.79 Å. A number of experimental points[14] are included. We see that the overall agreement is good, but discrepancies appear near the transition region. The calculated curves always show a marked drop in the annihilation rate, whereas the experimental points[14] tend to depart from the linear behavior in a smooth fashion. Note, however, that indications for a kinklike onset of Ps bubble formation in He have been reported at 4 and 30 K.[27] As discussed above, the translational degrees of freedom shift the transition to lower densities, making the drop smaller. Also, near the transition, fluctuations are likely to play a role; they are not included in the present mean-field-type approach. These are related to interesting questions about localization in a disordered system and, for example, a percolation model could be useful. Certainly the onset region of bubble formation deserves detailed theoretical and experimental studies.

The formation region of Ps bubbles is shown in Fig. 9. The experimental points are determined[14] by extrapolating through the points in Fig. 8 and finding where the line[27] corresponding to quasifree Ps is met. The calculated region where $\Delta\Omega < 0$ is somewhat smaller than the experimental one, as is evident already from Fig. 8. Here, again, threshold effects are important. If one roughly accounts for them by extrapolating also the calculated curves through the onset kink in a way similar to how the experimental phase boundary is determined, one arrives at the dotted curve in Fig. 9, in reasonably good agreement with experiment. Hernandez[12] has calculated the phase boundary $\Delta\Omega = 0$ using the ideal gas model for the fluid and either optical potential or hard-sphere Wigner-Seitz values for $E_\infty(n_0)$. Interpolating his results to a value of the scattering length of $a = 0.79$ Å, one obtains in the Wigner-Seitz case, a curve midway between the two in Fig. 9; the optical potential curve is lower, close to the experimental points.

Typical density profiles for Ps bubbles are given in Fig. 10. The temperature and density depen-

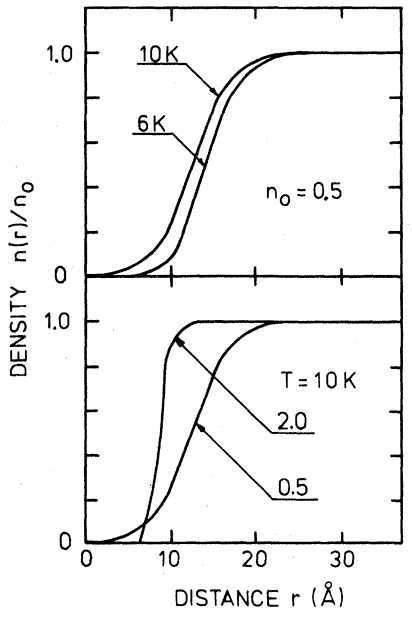

FIG. 10. The density profiles of Ps bubbles in helium at various temperatures and densities. Upper part: Fixed density $n_0 = 0.5 \times 10^{22}$ cm^{-3} with $T = 6$ and 10 K. Lower part: Fixed temperature $T = 10$ K with $n_0 = 2.0$ and 0.5×10^{22} cm^{-3}.

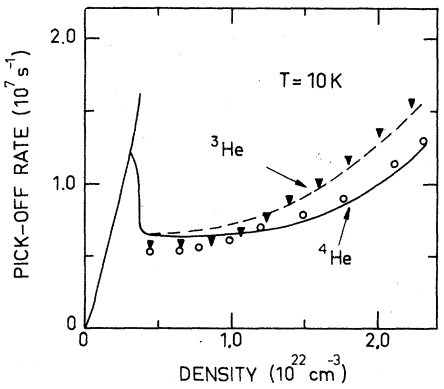

FIG. 11. The differences between the bubble-state pick-off rates of ortho-Ps in ^{3}He and ^{4}He. The ^{3}He result is obtained by scaling the helium hard-core diameter according to Eq. (35). Experimental points are from Ref. 14.

dence of these profiles is similar to that of the electron bubble. Note, however, that Ps bubbles are somewhat smaller in size than electron bubbles. In the electron case, the smaller mass leads to a higher zero-point pressure which is not compensated by the somewhat larger scattering length of Ps-He interaction.

The value of 0.79 Å for the Ps-He scattering length is a compromise giving an optimal fit to the experiment around 10 K. To check the effect of the equation of state, comparisons were made using the hard-sphere, van der Waals and Mann's[39] empirical equation of state in strictly local density-functional theory at $T = 10$ K. These indicate that a slightly smaller scattering length would improve the agreement at higher temperatures.

The situation at lower temperatures is not as clear since quantum effects are becoming important. In view of this the differences in behavior between the two isotopes of helium are of some interest. Above the λ point of ^{4}He the exchange effects are small. However, diffraction effects due to zero-point motion may be considerable, relating to the mass difference. Gibson[40] has investigated this problem and suggested that the helium hard-core diameter σ should be replaced by an effective one:

$$\sigma \to \sigma + \Lambda/2\sqrt{2}\,, \tag{35}$$

where $\Lambda = (2\pi\hbar^2/kTM_{\mathrm{He}})^{1/2}$ is the thermal wavelength. At 10 K this amounts for ^{3}He to a hard-core diameter of 2.69 Å which is 5% larger than that for ^{4}He. Since in our model the only difference between the two isotopes is the hard-core radius, it is interesting to see whether it can account for the differences between ^{3}He and ^{4}He. This is illustrated in Fig. 11. The experimental points are due to Hautojärvi *et al.*[14] We see that the increase in the hard-sphere diameter from 2.556 to 2.69 Å indeed fits well the differences between ^{3}He and ^{4}He. Thus we can qualitatively explain the isotope dependence. The quantitative validity of Eq. (35) in a wide temperature range is still to be explored. However, all quantum and temperature effects can be included in the theory outlined above by simply using the real structure factors for the fluids as soon as they are available.

VI. CONCLUSIONS

We have made a detailed density-functional study of excess electrons and positronium atoms in helium fluids. The theory explains much of the bubble formation data in a wide temperature and density range. However, discrepancies occur near the onset of bubble formation, where the need for a more sophisticated theory is indicated. A useful parametrization is presented for the Ps-He potential, and the isotope dependence of the Ps pick-off rate is shown to be consistent with the model. The formulation used is completely general and it will be interesting to apply the present methods to excess quantum particles in other fluids, notably heavier rare gases and hydrogen.

*Permanent address: Department of Physics, University of Jyväskylä, 40720 Jyväskylä, Finland.

[1]N. D. Lang, Solid State Phys. 28, 225 (1973).
[2]O. Gunnarsson and B. Lundquist, Phys. Rev. B 13, 4274 (1976).
[3]A. Ghazali and P. Leroux Hugon, Phys. Rev. Lett. 41, 1569 (1978).
[4]C. Ebner, W. F. Saam, and D. Stroud, Phys. Rev. A 14, 2264 (1976).
[5]R. A. Ferrell, Phys. Rev. 108, 167 (1957).
[6]H. T. Davis and R. G. Brown, Adv. Chem. Phys. 31, 329 (1975).
[7]P. Hautojärvi, K. Rytsölä, P. Tuovinen, A. Vehanen, and P. Jauho, Phys. Rev. Lett. 38, 842 (1977).
[8]M. J. Stott and E. Zaremba, Phys. Rev. Lett. 38, 1493 (1977).
[9]M. Manninen and P. Hautojärvi, Phys. Rev. B 17, 2129 (1978).
[10]For a review see, e.g., A. L. Fetter, in *The Physics of Liquid and Solid Helium*, edited by K. H. Bennemann and J. B. Ketterson (Wiley, New York, 1976) p. 242.
[11]C. Ebner and C. Punyanitya, Phys. Rev. A 19, 856 (1979).
[12]J. P. Hernandez, Phys. Rev. A 14, 1579 (1976).
[13]I. T. Iakubov and A. G. Khrapak, Appl. Phys. 16, 179 (1978).
[14]P. Hautojärvi, K. Rytsölä, and J. Vettenranta (unpublished).

[15]M. J. Stott and P. Kubica, Phys. Rev. B 11, 1 (1975).
[16]M. J. Stott and R. N. West, J. Phys. F 8, 635 (1978).
[17]P. A. Egelstaff, *An Introduction to the Liquid State* (Academic, London, 1967).
[18]N. R. Kestner, J. Jortner, M. H. Cohen, and S. A. Rice, Phys. Rev. A 140, 56 (1965).
[19]T. F. O'Malley, Phys. Rev. 130, 1020 (1963).
[20]L. Tankersley, J. Low Temp. Phys. 11, 451 (1973).
[21]J. P. Hernandez, Phys. Rev. B 11, 1289 (1975).
[22]R. L. Moore, C. L. Cleveland, and H. A. Gersch, Phys. Rev. B 18, 1183 (1978).
[23]H. A. Gersch, Phys. Rev. B 19, 1351 (1979).
[24]D. W. Gidley, A. Rich, P. W. Zitzewitz, and D. A. L. Paul, Phys. Rev. Lett. 40, 737 (1978).
[25]D. A. L. Paul and R. L. Graham, Phys. Rev. 106, 16 (1957).
[26]J. Wackerly and R. Stump, Phys. Rev. 106, 18 (1957).
[27]K. F. Canter, J. D. McNutt, and L. O. Roellig, Phys. Rev. A 12, 375 (1975); L. O. Roellig and T. M. Kelly, Phys. Rev. Lett. 18, 387 (1967).
[28]P. Hautojärvi, K. Rytsölä, P. Tuovinen, and P. Jauho, Phys. Lett. 57A, 175 (1976).
[29]J. B. Smith, Jr., J. D. McGervey, and A. J. Dahm, Phys. Rev. B 15, 1378 (1977).
[30]C. V. Briscoe, S.-I. Choi, and A. T. Stewart, Phys. Rev. Lett. 20, 493 (1968).
[31]J. P. Hernandez and S.-I. Choi, Phys. Rev. 188, 340 (1969).
[32]P. Hautojärvi, M. T. Loponen, and K. Rytsölä, J. Phys. B 9, 411 (1976).
[33]K. F. Canter and L. O. Roellig, Phys. Rev. A 12, 386 (1975).
[34]P. K. Tseng, S. Y. Chuang, S. H. Chen, and S. J. Tao, in *Proceedings of the Fifth International Conference on Positron Annihilation*, Lake Yamanaka, Japan, 1979 (in press).
[35]M. I. Barker and B. H. Bransden, J. Phys. B 1, 1109 (1968).
[36]P. Fraser, Proc. Phys. Soc (London) 78 328 (1961); *ibid.* 79, 721 (1962).
[37]R. J. Drachman and S. K. Houston, J. Phys. B 3, 1657 (1970).
[38]M. D. Miller (private communication).
[39]D. B. Mann, in *Technology of Liquid Helium*, U. S. Natl. Bur. Stand. Monograph No. 11, edited by R. H. Kropschot, B. W. Birmingham, and D. B. Mann (U. S. GPO, Washington D. C., 1968).
[40]W. G. Gibson, Mol. Phys. 30, 1 (1975); *ibid.* 30, 13 (1975).